HHS Public Access

Author manuscript

Dev Biol. Author manuscript; available in PMC 2019 February 01.

Published in final edited form as:

Dev Biol. 2018 February 01; 434(1): 74–83. doi:10.1016/j.ydbio.2017.11.013.

Gata6 restricts *Isl1* to the posterior of nascent hindlimb buds through *Isl1* cis-regulatory modules

Naoyuki Tahara[1,2], **Ryutaro Akiyama**[1,2,3], **Joshua W. M. Theisen**[4], **Hiroko Kawakami**[1,2], **Julia Wong**[1], **Daniel J. Garry**[4,5], and **Yasuhiko Kawakami**[1,2]

[1]Department of Genetics, Cell Biology and Development, University of Minnesota, Minneapolis, MN

[2]Stem Cell Institute, University of Minnesota, Minneapolis, MN

[4]Lillehei Heart Institute Regenerative Medicine and Sciences Program, University of Minnesota, Minneapolis, MN

[5]Paul and Sheila Wellstone Muscular Dystrophy Center, University of Minnesota, Minneapolis, MN

Abstract

Isl1 is required for two processes during hindlimb development: initiation of the processes directing hindlimb development in the lateral plate mesoderm and configuring posterior hindlimb field in the nascent hindlimb buds. During these processes, *Isl1* expression is restricted to the posterior mesenchyme of hindlimb buds. How this dynamic change in *Isl1* expression is regulated remains unknown. We found that two evolutionarily conserved sequences, located 3′ to the *Isl1* gene, regulate LacZ transgene expression in the hindlimb-forming region in mouse embryos. Both sequences contain GATA binding motifs, and expression pattern analysis identified that *Gata6* is expressed in the flank and the anterior portion of nascent hindlimb buds. Recent studies have shown that conditional inactivation of *Gata6* in mice causes hindlimb-specific pre-axial polydactyly, indicating a role of *Gata6* in anterior-posterior patterning of hindlimbs. We studied whether *Gata6* restricts *Isl1* in the nascent hindlimb bud through the cis-regulatory modules. *In vitro* experiments demonstrate that GATA6 binds to the conserved GATA motifs in the cis-regulatory modules. *GATA6* repressed expression of a luciferase reporter that contains the cis-regulatory modules by synergizing with *Zfpm2*. Analyses of *Gata6* mutant embryos showed that ISL1 levels are higher in the anterior of nascent hindlimb buds than in wild type. Moreover, we detected a greater number of *Isl1*-transcribing cells in the anterior of nascent hindlimb buds in *Gata6* mutants. Our results support a model in which *Gata6* contributes to repression of *Isl1* expression in the anterior of nascent hindlimb buds.

Correspondence to: Yasuhiko Kawakami, Ph.D., Department of Genetics, Cell Biology and Development, Stem Cell Institute, University of Minnesota, Minneapolis, MN. 55455, kawak005@umn.edu, Phone: 612-626-9935, Fax: 612-626-5652.

[3]Present address: Gene Regulation Research, Nara Institute of Science and Technology, Nara, Japan

Keywords

Isl1; *Gata6*; hindlimb buds; transcriptional regulation

INTRODUCTION

Isl1 encodes a LIM-homeodomain protein, which has diverse roles in the development of a variety of tissues and organs, such as the hindlimb (Kawakami et al., 2011; Narkis et al., 2012), pancreas (Ahlgren et al., 1997), retina (Elshatory et al., 2007), kidney (Kaku et al., 2013), motor neuron and interneuron (Pfaff et al., 1996; Song et al., 2009), mandibular arch (Li et al., 2017) and heart (Cai et al., 2003). Among these tissues/organs, *Isl1* has two functions specifically in hindlimbs: initiation of hindlimb buds (Kawakami et al., 2011) and setting up posterior hindlimb field in nascent hindlimb buds (Itou et al., 2012). During these processes, *Isl1* exhibits a dynamic expression pattern. *Isl1* is initially expressed in the posterior tip of the body at E8.5 (Cai et al., 2003). The expression extends in the posterior lateral plate mesoderm (LPM), where *Isl1* is required for the initiation of hindlimb development at E9.5 (Kawakami et al., 2011; Yang et al., 2006). During the early stages of hindlimb outgrowth, *Isl1* expression is restricted to the posterior hindlimb buds, and regulates the *Hand2-Shh* pathway (Itou et al., 2012). Thereafter, *Isl1* expression is rapidly downregulated. In contrast, *Isl1* expression was not detected in forelimb forming regions and in forelimb buds.

Given the functional importance of *Isl1* in development of various tissues and organs, several studies examined how *Isl1* expression is regulated during embryonic development. For instance, in the heart, *Isl1* is regulated by β-catenin signaling (Lin et al., 2007) and *Fgf8* - retinoic acid antagonism (Sirbu et al., 2008). At later stages, *Isl1* is regulated by *Shox2* in the sinoatrial node of the heart (Hoffmann et al., 2013). In the oral epithelium, BMP4 induces *Isl1* expression (Mitsiadis et al., 2003). However, it is unknown how the dynamic *Isl1* expression in the hindlimb progenitor cells is regulated.

Previous studies identified cis-regulatory modules for *Isl1* expression. A systematic screening by *in vitro* luciferase reporter assays and *in vivo* LacZ reporter transgenesis experiments lead to a conclusion that no tissue-specific cis-regulatory modules were located within 95 kb upstream sequence of the *Isl1* gene (Kappen and Salbaum, 2009). Instead, the same screening found a 10kb region covering exon 6, the last exon of the *Isl1* gene, and surrounding sequences drove tissue-specific LacZ reporter expression. The LacZ expression pattern recapitulated *Isl1* expression in the heart, visceral mesoderm and olfactory pit at E9.5–E10.5 (Kappen and Salbaum, 2009). Another study demonstrated that three conserved sequences, located 3′ to the *Isl1* gene, regulate LacZ reporter expression in the second heart field at E8.5 (Kang et al., 2009). Moreover, FOX family of the forkhead transcription factors directly regulated these conserved sequences. Despite these studies elucidating *Isl1* regulation in other organs and tissues, it remains unknown how *Isl1* expression in the hindlimb progenitors/nascent hindlimb bud mesenchyme is regulated.

Gata genes encode zinc finger DNA binding factors, and act as important regulators of tissue/organ development. The *Gata1/2/3* subfamily shows expression in hematopoietic cell

lineages, whereas the *Gata4/5/6* subfamily shows expression in the mesoendoderm lineages (Chlon and Crispino, 2012; Molkentin, 2000). Recent studies shed light on *Gata* gene functions in mouse limb development. Conditional inactivation of *Gata6* in the mesoderm caused preaxial polydactyly, the formation of extradigits in the anterior, specifically in hindlimbs (Hayashi et al., 2016; Kozhemyakina et al., 2014). These studies suggested two mechanisms of *Gata6* function in repressing *Shh* expression in the anterior hindlimb buds: GATA6 directly binds to and represses limb bud specific *Shh* enhancer (Kozhemyakina et al., 2014), and GATA6 promotes GLI3 repressor activities that repress *Shh* expression (Hayashi et al., 2016).

In this study, we found that the previously-characterized cardiac enhancers of the *Isl1* gene drives reporter expression in the hindlimb forming region in mouse embryos. The enhancer sequences contain GATA binding motifs. Among six *Gata* genes, we found that *Gata6* is transiently expressed in the flank and hindlimb-forming region, with a pattern complement to that of *Isl1*. We find GATA6 can bind the GATA motifs in the two conserved regions, and repress transcription *in vitro*. Furthermore, conditional deletion of *Gata6* caused upregulation of ISL1 and increased number of *Isl1*-transcribing cells in the anterior of hindlimb buds. Our data supports the idea that *Gata6* negatively regulates *Isl1*, and this regulation contributes to the posterior-biased *Isl1* expression.

MATERIALS AND METHODS

Mouse lines and in situ hybridization

Mice with the conditional allele of *Gata6* (*Gata6*^{fl}) and the *Tcre* deleter line have been described (Perantoni et al., 2005; Sodhi et al., 2006). *Tcre; Gata6*$^{fl/fl}$ mutant embryos were generated as previously described (Hayashi et al., 2016). Wild type mouse embryos were obtained by timed mating of CD-1 mice. Animal breeding was performed according to the approval by the Institutional Animal Care and Use Committee of the University of Minnesota. Whole mount in situ hybridization was done according to standard procedures (Itou et al., 2012).

LacZ reporter transgenesis

A 1.3 kb DNA fragment containing the CR, CR2 sequences and the sequence between them (Kang et al., 2009) was amplified from C57/BL6 genomic DNA, and subcloned into the hsp68-LacZ vector. The pronuclear injection of the expression cassette, whole mount LacZ staining at E9.5 and embryo genotyping were performed at Cyagen (http://www.cyagen.com/).

In vitro double strand oligo DNA pulldown assay

Flag-tagged full length human *GATA6* expression construct and a DNA-binding mutant form of *GATA6* were previously described (Zhong et al., 2011). HEK293T cells were transfected with *GATA6* expression constructs using the calcium phosphate transfection method. Cell extracts were passed through 25-gauge needle for extraction from the nucleus, and centrifuged at 8,000 g for 10 min at 4°C to remove debris. *In vitro* DNA binding assay was performed following a standard protocol (Ebert and Bunn, 1998; Nakayama et al.,

2002). In short, the supernatant was incubated with biotinylated double strand DNA at 4°C for 60 min, followed by incubation with Dynabeads M-280 Streptavidin (Invitrogen, Cat#11205D). After washing, proteins that bound to the double strand DNA were eluted into SDS-PAGE sample buffer, resolved by SDS-PAGE, transferred onto the PVDF membrane, and blotted with anti-FLAG M2 antibodies (Sigma, F3165, 1:1000 dilution).

The sequences of oligo DNAs are

CR1 wild type: ATTGTTGTTTTCTTGATAACCGAGCAAGCC and GGCTTGCTCGGTTATCAAGAAAACAACAAT.

CR1 GATA site mutant (lower cases represent mutated nucleotides): ATTGTTGTTTTCTTagTAACCGAGCAAGCC and GGCTTGCTCGGTTActAAGAAAACAACAAT

CR2 wild type: CTGGTGGCTCGGCGGCTCCTTATCTTTCCC and GGGAAAGATAAGGAGCCGCCGAGCCACCAG

CR2 GATA site mutant: CTGGTGGCTCGGCGGCTCCTTActTTTCCC and GGGAAAagTAAGGAGCCGCCGAGCCACCAG

Electrophoretic mobility shift assay

GATA6, mutant *GATA6*, or empty pcDNA3.1(+)-HA vector were expressed using the TNT Quick Coupled Transcription/Translation System (Promega, Madison, WI) according to the manufacturer's protocol. Oligo DNA corresponding to wild-type or mutant CR1 and CR2 (the same sequences as oligo DNA pulldown assay) were synthesized with and without the IRDye® 700 fluorophore (Integrated DNA Technologies, Coralville, IA) and annealed to generate labeled probes and unlabeled competitor DNA. *In vitro* synthesized protein (2 μL) was incubated with 1 μg of poly dI-dC in binding buffer (10 mM Tris pH 8.0, 50 mM sodium chloride, 1 mM EDTA, 5 mM DTT, 5 mM MgCl2, 1 mg/ml BSA) at room temperature for 10 minutes. For antibody treatment, pre-binding was performed in the presence of active or heat-inactivated anti-human GATA6 antibody (AF1700, R&D Systems Inc.). IRDye® 700-labelled probe (100 fmol) was then added and the binding reaction proceeded at room temperature for 15 minutes. DNA-protein complexes were resolved on a 6% non-denaturing polyacrylamide gel in 0.5x TBE (40 mM Tris pH 8.3, 45 mM boric acid, and 1 mM EDTA) at room temperature. Fluorescence was detected using an Odyssey CLx imager (LI-COR Biosciences, Lincoln, NE).

In vitro luciferase reporter assay

The *Isl1*-luciferase reporter was generated by cloning the 1.3 kb genomic DNA fragment, covering the CR1 to CR2 region, into a thymidine kinase minimum promoter-luciferase vector. NIH3T3 cells were plated at 3×10^4/well into a 48-well plate, and transiently transfected with the *Isl1*-luciferase reporter (100 ng), Renilla luciferase construct (5 ng) and expression constructs (50 ng) using Fugene 6 (Promega). Luciferase activities were measured 40–44 hours after transfection using the Dual Luciferase Reporter Assay System (Promega). Experiments were performed in triplicate, and the results are shown as average ±

standard deviation. Statistical significance was determined by One-way ANOVA with post-hoc Tukey HSD test.

Immunofluorescence and image analysis

For immunofluorescence, embryos were fixed in 4% PFA at 4°C for 2 hours, washed with cold PBS three times and embedded in OCT compound. For GATA1 expression analysis, transverse cryosections (14 μm thickness) of tissues at 25th somite levels or posterior were stained without epitope retrieval using goat anti-GATA1 (sc-1234, Sant Cruz, 1:100 dilution) together with either rat anti-TER-119 (#116201, BioLegend, 1:100 dilution) or rabbit anti-SOX2 (AB5603, Millipore, 1:500 dilution). Secondary antibodies used were Alexa 594 donkey anti-goat IgG (A-11058, Invitrogen, 1:500 dilution), Rhodamine Red-X donkey anti-rat IgG (#712-295-153, Jackson Immuno Research, 1:250 dilution) and Rhodamine Red-X donkey anti-rabbit IgG (#711-295-152, Jackson Immuno Research, 1:250 dilution). Fluorescent images were acquired by Zeiss LSM710 laser microscopy and analyzed by ZEN software.

For ISL1 and GATA6 signal analysis, coronal cryosections of the hindlimb forming regions and nascent hindlimb buds were made at 14 μm thickness. Immunostaining was done without epitope retrieval procedures. Primary antibodies used were mouse anti-ISL1 (39.4D5, Developmental Studies Hybridoma Bank, 4.03 μg/ml) and goat anti-GATA6 (AF1700, R&D Systems Inc, 5 μg/ml) antibodies. Secondary antibodies used were Alexa 488 donkey anti-mouse IgG and Alexa 594 donkey anti-goat IgG (Invitrogen, 1:500 dilution). Images were acquired by Zeiss LSM710 and analyzed by ZEN software. From each embryo, 3–5 sections were stained, and the section representative of the lateral plate mesoderm was chosen for image analysis.

Fluorescent *in situ* hybridization and Imaris imaging analysis

Digoxigenin-labelled antisense *Isl1* intron probe (1200 bp in the intron 4 sequence) was synthesized, and *in situ* hybridization was performed with modifications to a standard protocol (Itou et al., 2012). After washing procedures in day 2, peroxidase-labelled anti-DIG (Sigma, Cat#11207733910, SIGMA, 1:300 dilution) was used instead of alkaline phosphatase-labelled anti-DIG, and the Tyramide Signal Amplification kit #2 (Alexa Fluor 488, Invitrogen) was used to develop fluorescent signals. For the quantification of *Isl1* FISH signals, confocal image stacks were acquired as 16 Bit images of the lateral view of hindlimb forming region/nascent hindlimb bud using Zeiss LSM710 laser microscopy. The images were analyzed using the spots function of the Imaris v7.6.4 (Bitplane). We input the 25th to 29th somite area (hindlimb buds) as the Region of Interest. At 26 and 28 somite stages, we defined prospective somite levels to 29th somite, based on the size of 2–3 pairs of newly formed somites. Microsoft excel was used to create the final bar charts.

RESULTS

The CR1 and CR2 enhancers of Isl1 drive expression of LacZ reporter in hindlimb forming region

Previous studies have identified cardiac *Isl1* enhancers located between 3324 and 6965 bp downstream of the translational stop codon in the mouse *Isl1* gene. This sequence contains three conserved sequences, CR1, CR2 and CR3 (Fig. 1A) (Kang et al., 2009; Kappen and Salbaum, 2009). Among three conserved regions, the CR2 sequence is shown to be critical for LacZ reporter expression in the pharyngeal mesoderm in E8.5 embryos. We compared this region among species and found that CR1 and CR2 are highly conserved among human, mouse, chick and *Xenopus*, while CR3 is less conserved in *Xenopus*. Zebrafish possess pectoral fins and pelvic fins as counter parts of forelimbs and hindlimb, respectively. However, the zebrafish sequence did not exhibit conservation to the three conserved sequences. Whether this region contributes to expression of *Isl1* in the hindlimb forming region is still unknown. Because the CR3 sequence has lower levels of conservation, we tested the activity of the CR1+CR2 region by transient LacZ transgenesis in mouse embryos (Fig. 1B). For this purpose, we cloned 1.3 kb fragment that contains CR1 to CR2, including the sequence between them. We detected LacZ staining in the hindlimb forming region at E9.5 (Fig. 1D, E, n=3/5). The signals were also detected in the mandibular arch, where *Isl1* is also expressed at this stage. These LacZ expression patterns are similar to but broader than endogenous *Isl1* expression pattern at E9.5 (Fig. 1C) (Akiyama et al., 2014; Kawakami et al., 2011; Yang et al., 2006; Zhuang et al., 2013). The broader expression pattern of LacZ reporter may be due to the stability of LacZ protein than *Isl1* mRNA. In contrast, the LacZ reporter was not detected in the motor neuron, where endogenous *Isl1* mRNA was detected (Fig. 1C, D). These results demonstrate that the conserved CR1 and CR2 sequences contribute to expression of *Isl1* in hindlimb progenitors.

Gata6 is transiently expressed in the hindlimb-forming region and hindlimb buds

By sequence analysis using Jaspear database (http://jaspar.genereg.net/), we found that both CR1 and CR2 contain GATA transcription factor binding motifs (Fig. S1). In order to figure out whether *Gata* genes are involved in regulation of the CR1-CR2 sequence, we performed *in situ* hybridization of all *Gata* genes at E9.5 (25–26 somite stage). *Gata1* was expressed in the hindlimb forming region in a speckled manner, suggesting that migrating hematopoietic cells express *Gata1* (Fig. 2A). In order to confirm *Gata1* expression in hematopoietic cells, we performed immunofluorescence analysis of transverse section of 25-somite stage embryos. GATA1 was co-detected with TER-119, a blood cell marker (Kina et al., 2000) (Fig. 2G). Since blood cells tend to generate non-specific signals under fluorescence detection, we also simultaneously detected GATA1 and a neural marker SOX2. While SOX2 signals were detected in the neural tube, it was not detected in GATA1-positive cells (Fig. 2H). Therefore, hematopoietic cells in the lateral plate mesoderm at E9.5 express GATA1.

Although *Gata2* was expressed in the lateral nasal prominence at E9.5 (Fig. 2I) and both medial and lateral nasal prominences at E10.5 (Fig. 2J), *Gata2* was not detected in the hindlimb forming region (Fig. 2B). *Gata3* expression was detected in the intermediate mesoderm and 3rd pharyngeal pouch (Fig. 2C, K), as previously reported (Manaia et al.,

2000); however, we did not detect *Gata3* expression in the hindlimb forming region (Fig. 2C). Strong expression of *Gata4* was detected broadly in the developing heart (Fig. 2L) (Auda-Boucher et al., 2000), and weak expression of *Gata5* was detected in the ventricle and outflow tract (Fig. 2M) (Morrisey et al., 1997). However, we did not detect expression of *Gata4* and *Gata5* in the hindlimb forming region (Fig. 2D, E). In contrast to these observations, we found that *Gata6* is expressed in the trunk and hindlimb forming region (Fig. 2F).

Our recent study showed that *Gata6* is expressed in the anterior portion of hindlimb buds at E10.25 (34 somite stage) (Hayashi et al., 2016); however, *Gata6* expression pattern between E9.5 and E10.0 remained unknown. Therefore, next we compared expression pattern of *Isl1* and *Gata6* in more detail during E9.5–E10.0. As previously analyzed (Itou et al., 2012), *Isl1* expression was detected in the hindlimb forming region at 24 somite stage (Fig. 3E), and the expression is localized to the posterior of the hindlimb bud during hindlimb budding (26–28 somite stages, Fig. 3F, G). At E10.0 (30 somite stage), *Isl1* expression becomes very faint in hindlimb buds (Fig. 3H). *Gata6* was detected in the flank at 24 somite stage (Fig. 3A), and the expression extends into the anterior portion of hindlimb buds at 26–28 somite stages (Fig. 3B, C). The expression is localized to the anterior margin of hindlimb buds at E10.0 (30 somite, Fig. 3D). These complementary expression patterns of *Isl1* and *Gata6* suggest that *Gata6* excludes *Isl1* from the anterior portion of the hindlimb bud.

Gata6 binds to the GATA binding motifs in the CR1 and CR2 sequences and represses gene expression in vitro

Given that CR1 and CR2 possess consensus GATA-binding sequences, we next examined whether GATA6 can bind these consensus sequences by an *in vitro* DNA binding assay. Biotinylated double strand oligo DNA was incubated with FLAG-tagged GATA6-transfected cell extract. The oligo DNA-protein complex was pulled down by Streptavidin-beads, and bound protein was resolved and detected by anti-FLAG Western blotting. GATA6 bound to the consensus sequences in both CR1 and CR2, with stronger band to the CR2 oligo (Fig. 4A). Introducing point mutations in two bases in the consensus GATA motifs significantly reduced GATA6 binding. Moreover, mutant GATA6, in which key amino acid residues in the DNA binding domain of GATA6 were mutated (Zhong et al., 2011), only exhibited background signals, confirming the specific binding of GATA6 to the consensus sequences in CR1 and CR2.

In order to further characterize GATA6 binding to the consensus motifs in the CR1 and CR2 sequences, we also performed EMSA assay. *In vitro*-translated GATA6 bound both CR1 and CR2 oligos, which was detected as a shift of bands (indicated by an arrowhead in Fig. 4B). Similar to the oligo DNA pulldown experiment, mutant GATA6 did not show binding to CR1 and CR2 oligos. Pre-incubating GATA6 with anti-GATA6 antibodies, but not with heat-inactivated (h.i.) antibodies, abolished the band shift, indicating that the shift of CR1 and CR2 probe oligos is due to GATA6 binding. We next tested specificity of GATA6 binding by using wild type and mutant forms of CR1 oligos and CR2 oligos as competitors. Pre-incubation of excess amount (50 fold) of wild type competitors significantly reduced the mobility shift of CR1 and CR2 oligos, while mutant competitors did not affect GATA6-

probe complex (Fig. 4C). This result confirmed the sequence specificity of GATA6 binding to CR1 and CR2 oligos. Because GATA6 binds to both CR1 and CR2 sequences, we further tested whether GATA6 has different affinities to CR1 or CR2. We incubated GATA6, CR1 probe and various amounts of competitors, and the GATA6-probe complex was resolved (Fig. 4D). Then, we detected GATA6-CR1 probe band intensities, relative to the intensities of the same area without GATA6 (left-most lane in Fig. 4D). When CR2 oligos were used as competitors, the band intensities were slightly lower than that with CR1 oligos as competitors (Fig. 4E). These data suggest that GATA6 may have slightly higher affinity for CR2 than for CR1 sequences; however, the differences are minor.

The results obtained by two *in vitro* approaches (oligo DNA pulldown and EMSA) support the idea that GATA6 can bind to consensus GATA motifs in the CR1 and CR2 sequences.

Next, we asked whether the binding of GATA6 contributes to transcriptional regulation. For this purpose, we used *in vitro* luciferase reporter assays. We transfected NIH3T3 cells with a luciferase reporter that contains thymidine kinase minimum promoter and 1.3 kb genomic region that contains CR1 to CR2 sequence together with various expression constructs (Fig. 5A). *GATA6*, mutant *GATA6* and *Zfpm2* (also known as *Fog2*), which modulate the activities of GATA proteins (Chlon and Crispino, 2012), did not exhibit significant activities (Fig. 5B). In contrast, *GATA6*, but not mutant *GATA6*, synergized with *Zfpm2*, and repressed the reporter activities. These results indicate that *GATA6* cooperates with *Zfpn2* and represses transcription through CR1 and CR2 sequences.

Loss of Gata6 causes upregulation of ISL1 in the anterior hindlimb bud

The results we obtained support the hypothesis that *Gata6* contributes to repression of *Isl1* in the anterior of the nascent hindlimb bud. If this is the case, we would expect anteriorly expanded *Isl1* expression in *Gata6* mutant embryos. For this purpose, we used *Tcre* to conditionally inactivate the *Gata6* gene, given efficient recombination by *Tcre* (Perantoni et al., 2005). We simultaneously detected ISL1 and GATA6 immunoreactivities in coronal sections of the nascent hindlimb bud at the 28 somite stage. We examined three wild type and three *Gata6* mutant embryos. Among the three to five sections stained per embryo, we selected the section representing the hindlimb bud along the anterior-posterior axis from each embryo. Along the anterior-posterior axis, we detected GATA6 and ISL1 signals (Fig. 6A–H), and plotted their fluorescent intensities. Fig. 6I shows plots along the anterior-posterior axis in wild type, in which relative signal intensities are shown such that the maximum GATA6 signals and the maximum ISL1 signals in a section is set 1.0 signal intensity. This plotting allows for evaluation of changes in intensity of GATA6 or ISL1 in a section. The GATA6 signals were higher in the anterior portion and the signal intensity was reduced towards the posterior part (Fig. 6B, I). ISL1 signals were high in the posterior, and the signal declined in the middle to the anterior of hindlimb buds (Fig. 6C, I). These signal intensities exhibited reverse correlations, supporting the idea that GATA6 represses *Isl1*.

In *Tcre; Gata6*$^{fl/fl}$ mutants, the GATA6 signals were at the background levels, confirming the efficient deletion by *Tcre* (Fig. 6F). We compared relative ISL1 signal intensities in wild type and *Tcre; Gata6*$^{fl/fl}$ mutants. The graph presented as Fig. 6J shows relative ISL1 signal intensity within either wild type or *Tcre; Gata6*$^{fl/fl}$ section, not comparison of relative signal

intensities between wild type and *Tcre; Gata6*$^{fl/fl}$ sections. In this graph, the position of the highest relative peak intensities of ISL1 signals in the *Tcre; Gata6*$^{fl/fl}$ section shifted anteriorly, compared to the position of the highest peak intensities of ISL1 in the wild type section. Moreover, relative ISL1 signal intensities in the anterior, compared to the highest intensity within each section, were higher in the *Tcre; Gata6*$^{fl/fl}$ section. This relative increase in the ISL1 signal intensity in the anterior is in contrast to the sharp drop of the ISL1 signal intensity in the anterior of the wild type section. These results support the hypothesis that *Gata6* contributes to repression of *Isl1* in the anterior of the nascent hindlimb bud.

Loss of Gata6 causes increased number of cells that transcribe Isl1 in the anterior hindlimb bud

In addition to immunofluorescence analysis of ISL1, we sought to determine *Gata6* regulation on *Isl1* transcription *in vivo*. For this purpose, we used an intron probe for *in situ* hybridization. Previous studies indicated that detection of intronic transcript provides advantages (Dubrulle and Pourquie, 2004; Ibanes et al., 2006): First, it allows for detecting cells in which *Isl1* is being transcribed. In rapidly dividing cells, such as early limb bud cells, cellular contents, such as mature mRNA, could be inherited to daughter cells that had shut off transcription of specific genes (Dubrulle and Pourquie, 2004; Ibanes et al., 2006). Therefore, this method would be suitable to evaluate the loss of *Gata6* on *Isl1* transcription. Second, nuclear fluorescent signals of intronic probes offer higher image resolution than detecting mature mRNA in cytoplasm, allowing for quantitating number of *Isl1* transcribing cells.

By coupling a conventional *in situ* hybridization method using an *Isl1* intron probe with the Tyramide Signal Amplification system (Neufeld et al., 2013), we detected nascent *Isl1* transcripts as fluorescent signals, and acquired images by confocal microscopy (Fig. 7A, B, D, E, I, J). We focused our analysis to the nascent hindlimb buds (25th–29th somite area). When somites are not yet developed yet, we predicted somite positions based on the size of 2–3 pairs of most posterior somites. In order to quantify number of cells that are transcribing *Isl1*, we converted each *Isl1*-positive signal (i.e. a nucleus in which premature *Isl1* transcripts are present) into a dot in the image by using the Imaris software. Then, we counted *Isl1*-transcribing cell number in every 20 μm width in the lateral view. (Fig. 7C, F–H, K).

In wild type embryos, the number of *Isl1*-transcribing cells increased from the anterior to posterior order, peaked in the 28th somite level, and then dropped in 28 somite stage embryos (Fig. 7D, F, G). Between 25th and the putative 29th somite levels, the average number of *Isl1*-transcribing cells in 20 μm width was 48.5 (Fig. 7G). In contrast, in *Tcre; Gata6*$^{fl/fl}$ hindlimb buds the average number of *Isl1*-transcribing cells in 20 μm width became 64.2 (Fig. 7H). When comparing the number in each pair of 20 μm width at the same position, the number of *Isl1*-transcribing cells was significantly higher in 25th and 26th somite levels in *Tcre; Gata6*$^{fl/fl}$ hindlimb buds (Fig. 7F). These results support the idea that *Gata6* represses *Isl1* expression. This difference in the number of *Isl1*-transcribing cells was not observed at 26 somite stage. At 30 somite stage when endogenous *Isl1* expression is

downregulated, the number of *Isl1*-transcribing cells was similar between the 26–28 somite levels in both wild type and *Tcre; Gata6*$^{fl/fl}$ hindlimb buds (Fig. 7I, J, K). At this stage, we detected a greater number of *Isl1*-transcribing cells only in the 25th somite level in *Tcre; Gata6*$^{fl/fl}$ hindlimb buds, compared to wild type. These results suggest that *Gata6*-dependent *Isl1* repression is stage specific, and collectively support the idea that *Gata6* contributes to repression of *Isl1* in the anterior of the nascent hindlimb bud.

DISCUSSION

Accumulating reports indicate that forelimbs and hindlimbs utilize distinct genetic systems, upstream of common patterning processes, to regulate their development (Tao et al., 2017). Two early steps of limb development, namely limb initiation and pre-patterning, illustrate such limb-type specific differences. *Isl1* plays important roles during both processes (Itou et al., 2012; Kawakami et al., 2011). After hindlimb buds begin outgrowth, *Isl1* expression is rapidly restricted to the posterior, where *Isl1* acts upstream of the *Hand2-Shh* pathway. Our data support the idea that *Gata6* contributes to posterior restriction of *Isl1* expression through CR1 and CR2 cis-regulatory modules, located in the 3′ of the *Isl1* gene.

Tissue-type specific Isl1 regulations through cis regulatory modules

Isl1 expression is detected in a variety of tissues/cell types during embryonic development. A previous study demonstrated that a 3.6 kb sequence, spanning CR1, CR2 and a less conserved CR3, drive LacZ reporter expression in the second heart field and its derivative at E8.5–E9.75 (Kang et al., 2009). This LacZ expression recapitulated endogenous *Isl1* expression in the heart. Deletion analysis indicated that CR1 has variable activities, and CR2 exhibits consistent and robust activities to drive LacZ transgene, while CR3 did not show the activities. Our transgene construct that contains both CR1 and CR2 drove LacZ reporter expression in the hindlimb forming region and mandibular arch at E9.5, where *Isl1* is expressed (Akiyama et al., 2014; Kawakami et al., 2011; Zhuang et al., 2013). *Isl1* is also expressed in the motor neuron at E9.5 (Pfaff et al., 1996). A recent study identified two motor-neuron-specific *Isl1* enhancers, distantly located from the *Isl1* gene (Kim et al., 2015). These studies highlight two distinct regulations of *Isl1* expression: The closely located enhancer that contains CR1 and CR2 sequences regulate *Isl1* expression in the hindlimb-forming region, heart, mandibular arch, while neural expression of *Isl1* is regulated by two distantly located sequences.

Role of Gata6 as a repressor of developmental genes

A previous study demonstrated that CR2 is the most critical region among the three CR sequences for expression in the second heart field. *In vitro* DNA binding assay demonstrated that FOX family transcription factors directly regulate CR2 activities (Kang et al., 2009). We found that both CR1 and CR2 contain GATA binding motifs (Figure S1), and our results support the idea that *Gata6* acts as a repressor and contributes to the repression of *Isl1* in the anterior of nascent hindlimb buds. Recent studies showed that *Gata6* acts as a repressor in developing hindlimb buds (Kozhemyakina et al., 2014). GATA6 binds to oligo DNAs that possesses the *Gli1* promoter sequence, and GATA6 blocked GLI1-dependent activation of *Gli1*-luciferase reporter expression *in vitro. Gata6* also repressed *Hand2* and *Hoxd13*-

dependent activation of *Shh* enhancer-luciferase *in vitro*. These repressive activities were enhanced in the presence of *Zfpm2*. In our assay, *GATA6* or *Zfpm2* alone did not exhibit repressive activities on *Isl1* enhancer luciferase; however, *GATA6* plus *Zfpm2* could repress the reporter (Fig. 5B). ZFPM2 is known to bind to the transcriptional corepressors, such as NuRD (Chlon and Crispino, 2012). Therefore, repression by GATA6 *in vivo* would also require interaction with ZFPN2.

Gata6 contributes to repression of Isl1 in the anterior of the nascent hindlimb bud

Our analyses of ISL1 levels and number of *Isl1*-transcribing cells in *Tcre; Gata6*$^{fl/fl}$ embryos support our hypothesis that *Gata6* contributes to repression of *Isl1* in the anterior hindlimb buds *in vivo*. In the first set of data (ISL1 levels), immunofluorescence show levels of ISL1 signals. In wild type embryos, ISL signals and GATA6 signals showed a reciprocal pattern. In addition, relative signal intensity of ISL1 became higher in the anterior-middle region of the nascent hindlimb buds of *Tcre; Gata6*$^{fl/fl}$ embryos (Fig. 6J). This result is consistent with our hypothesis that *Gata6* restricts *Isl1* expression to the posterior of hindlimb buds. In the second set of analysis, we detected *Isl1*-transcribing cells by means of intron probe *in situ* hybridization (Fig. 7). The use of intron-probe provided spatial resolution to detect nascent RNA prior to processing. Conversion of fluorescent signals by the Imaris software allowed for counting *Isl1*-transcribing cells for quantitative analysis. This approach provided evidence that number of *Isl1*-transcribing cells is greater in the nascent hindlimb bud at 28 somite stage in *Tcre; Gata6*$^{fl/fl}$ than in wild type. This result is also supports our hypothesis.

The increase in the number of *Isl1*-transcribing cells in *Tcre; Gata6*$^{fl/fl}$ embryos was most evident at the 28 somite stage. The number of *Isl1*-transcribing cells was reduced in both wild type and *Tcre; Gata6*$^{fl/fl}$ hindlimb buds at the 30 somite stage, and *Isl1* expression is eventually downregulated from hindlimb buds of both wild type and *Tcre; Gata6*$^{fl/fl}$ hindlimb buds. This result suggests that other mechanisms also regulate spatial-temporal *Isl1* expression in the hindlimb buds. Such mechanisms are still to be uncovered for detailed understanding of regulation of *Isl1* expression in hindlimb buds. Nonetheless, our results collectively support the idea that *Gata6* represses *Isl1*, which contributes to restricting *Isl1* expression to posterior hindlimb buds.

Supplementary Material

Refer to Web version on PubMed Central for supplementary material.

Acknowledgments

We are grateful to Shinichi Hayashi, Junji Itou, Sho Kawakami, Jennifer Kim, Jenna Matson, Avery Swearer and Samantha Young for their excellent technical assistance and advices, and to Malina Yamashita Peterson for editorial assistance. We also thank Dr. Yi Zhong and Dr. Christine Iacobuzio-Donahue for human *GATA6* expression constructs, Dr. Naoko Koyano-Nakagawa for the *Zfpm2* expression construct, Dr. Stephanie Ware for the TK-minimum promoter luciferase vector, Dr. Takaaki Matsui for the oligo DNA pulldown assay protocol, and Dr. Naoyuki Wada for critical reading of the manuscript. This study was supported by grants from the National Institute of Arthritis, Musculoskeletal and Skin Diseases to YK (R01AR064195, R21AR063782) and the National Heart, Lung, and Blood Institute to DJG (R01HL122576). The funders had no role in study design, data collection and analysis, decision to publish, or preparation of the manuscript. The authors have no conflicts to disclose.

References

Ahlgren U, Pfaff SL, Jessell TM, Edlund T, Edlund H. Independent requirement for ISL1 in formation of pancreatic mesenchyme and islet cells. Nature. 1997; 385:257–260. [PubMed: 9000074]

Akiyama R, Kawakami H, Taketo MM, Evans SM, Wada N, Petryk A, Kawakami Y. Distinct populations within Isl1 lineages contribute to appendicular and facial skeletogenesis through the beta-catenin pathway. Developmental biology. 2014; 387:37–48. [PubMed: 24424161]

Auda-Boucher G, Bernard B, Fontaine-Perus J, Rouaud T, Mericksay M, Gardahaut MF. Staging of the commitment of murine cardiac cell progenitors. Developmental biology. 2000; 225:214–225. [PubMed: 10964476]

Cai CL, Liang X, Shi Y, Chu PH, Pfaff SL, Chen J, Evans S. Isl1 identifies a cardiac progenitor population that proliferates prior to differentiation and contributes a majority of cells to the heart. Developmental cell. 2003; 5:877–889. [PubMed: 14667410]

Chlon TM, Crispino JD. Combinatorial regulation of tissue specification by GATA and FOG factors. Development (Cambridge, England). 2012; 139:3905–3916.

Dubrulle J, Pourquie O. fgf8 mRNA decay establishes a gradient that couples axial elongation to patterning in the vertebrate embryo. Nature. 2004; 427:419–422. [PubMed: 14749824]

Ebert BL, Bunn HF. Regulation of transcription by hypoxia requires a multiprotein complex that includes hypoxia-inducible factor 1, an adjacent transcription factor, and p300/CREB binding protein. Molecular and cellular biology. 1998; 18:4089–4096. [PubMed: 9632793]

Elshatory Y, Everhart D, Deng M, Xie X, Barlow RB, Gan L. Islet-1 controls the differentiation of retinal bipolar and cholinergic amacrine cells. J Neurosci. 2007; 27:12707–12720. [PubMed: 18003851]

Hayashi S, Akiyama R, Wong J, Tahara N, Kawakami H, Kawakami Y. Gata6-Dependent GLI3 Repressor Function is Essential in Anterior Limb Progenitor Cells for Proper Limb Development. PLoS Genet. 2016; 12:e1006138. [PubMed: 27352137]

Hoffmann S, Berger IM, Glaser A, Bacon C, Li L, Gretz N, Steinbeisser H, Rottbauer W, Just S, Rappold G. Islet1 is a direct transcriptional target of the homeodomain transcription factor Shox2 and rescues the Shox2-mediated bradycardia. Basic Res Cardiol. 2013; 108:339. [PubMed: 23455426]

Ibanes M, Kawakami Y, Rasskin-Gutman D, Belmonte JC. Cell lineage transport: a mechanism for molecular gradient formation. Molecular systems biology. 2006; 2:57. [PubMed: 17047664]

Itou J, Kawakami H, Quach T, Osterwalder M, Evans SM, Zeller R, Kawakami Y. Islet1 regulates establishment of the posterior hindlimb field upstream of the Hand2-Shh morphoregulatory gene network in mouse embryos. Development (Cambridge, England). 2012; 139:1620–1629.

Kaku Y, Ohmori T, Kudo K, Fujimura S, Suzuki K, Evans SM, Kawakami Y, Nishinakamura R. Islet1 Deletion Causes Kidney Agenesis and Hydroureter Resembling CAKUT. J Am Soc Nephrol. 2013:24. In Press.

Kang J, Nathan E, Xu SM, Tzahor E, Black BL. Isl1 is a direct transcriptional target of Forkhead transcription factors in second-heart-field-derived mesoderm. Developmental biology. 2009; 334:513–522. [PubMed: 19580802]

Kappen C, Salbaum JM. Identification of regulatory elements in the Isl1 gene locus. The International journal of developmental biology. 2009; 53:935–946. [PubMed: 19598113]

Kawakami Y, Marti M, Kawakami H, Itou J, Quach T, Johnson A, Sahara S, O'Leary DD, Nakagawa Y, Lewandoski M, Pfaff S, Evans SM, Izpisua Belmonte JC. Islet1-mediated activation of the beta-catenin pathway is necessary for hindlimb initiation in mice. Development (Cambridge, England). 2011; 138:4465–4473.

Kim N, Park C, Jeong Y, Song MR. Functional Diversification of Motor Neuron-specific Isl1 Enhancers during Evolution. PLoS Genet. 2015; 11:e1005560. [PubMed: 26447474]

Kina T, Ikuta K, Takayama E, Wada K, Majumdar AS, Weissman IL, Katsura Y. The monoclonal antibody TER-119 recognizes a molecule associated with glycophorin A and specifically marks the late stages of murine erythroid lineage. Br J Haematol. 2000; 109:280–287. [PubMed: 10848813]

Kozhemyakina E, Ionescu A, Lassar AB. GATA6 is a crucial regulator of Shh in the limb bud. PLoS Genet. 2014; 10:e1004072. [PubMed: 24415953]

Li F, Fu G, Liu Y, Miao X, Li Y, Yang X, Zhang X, Yu D, Gan L, Qiu M, Chen Y, Zhang Z, Zhang Z. 2017ISLET1-Dependent beta-Catenin/Hedgehog Signaling Is Required for Outgrowth of the Lower Jaw. Molecular and cellular biology. :37.

Lin L, Cui L, Zhou W, Dufort D, Zhang X, Cai CL, Bu L, Yang L, Martin J, Kemler R, Rosenfeld MG, Chen J, Evans SM. Beta-catenin directly regulates Islet1 expression in cardiovascular progenitors and is required for multiple aspects of cardiogenesis. Proceedings of the National Academy of Sciences of the United States of America. 2007; 104:9313–9318. [PubMed: 17519333]

Manaia A, Lemarchandel V, Klaine M, Max-Audit I, Romeo P, Dieterlen-Lievre F, Godin I. Lmo2 and GATA-3 associated expression in intraembryonic hemogenic sites. Development (Cambridge, England). 2000; 127:643–653.

Mitsiadis TA, Angeli I, James C, Lendahl U, Sharpe PT. Role of Islet1 in the patterning of murine dentition. Development (Cambridge, England). 2003; 130:4451–4460.

Molkentin JD. The zinc finger-containing transcription factors GATA-4, -5, and -6. Ubiquitously expressed regulators of tissue-specific gene expression. The Journal of biological chemistry. 2000; 275:38949–38952. [PubMed: 11042222]

Morrisey EE, Ip HS, Tang Z, Lu MM, Parmacek MS. GATA-5: a transcriptional activator expressed in a novel temporally and spatially-restricted pattern during embryonic development. Developmental biology. 1997; 183:21–36. [PubMed: 9119112]

Nakayama K, Kim KW, Miyajima A. A novel nuclear zinc finger protein EZI enhances nuclear retention and transactivation of STAT3. The EMBO journal. 2002; 21:6174–6184. [PubMed: 12426389]

Narkis G, Tzchori I, Cohen T, Holtz A, Wier E, Westphal H. Isl1 and Ldb co-regulators of transcription are essential early determinants of mouse limb development. Dev Dyn. 2012; 241:787–791. [PubMed: 22411555]

Neufeld SJ, Zhou X, Vize PD, Cobb J. mRNA fluorescence in situ hybridization to determine overlapping gene expression in whole-mount mouse embryos. Dev Dyn. 2013; 242:1094–1100. [PubMed: 23749471]

Perantoni AO, Timofeeva O, Naillat F, Richman C, Pajni-Underwood S, Wilson C, Vainio S, Dove LF, Lewandoski M. Inactivation of FGF8 in early mesoderm reveals an essential role in kidney development. Development (Cambridge, England). 2005; 132:3859–3871.

Pfaff SL, Mendelsohn M, Stewart CL, Edlund T, Jessell TM. Requirement for LIM homeobox gene Isl1 in motor neuron generation reveals a motor neuron-dependent step in interneuron differentiation. Cell. 1996; 84:309–320. [PubMed: 8565076]

Sirbu IO, Zhao X, Duester G. Retinoic acid controls heart anteroposterior patterning by down-regulating Isl1 through the Fgf8 pathway. Dev Dyn. 2008; 237:1627–1635. [PubMed: 18498088]

Sodhi CP, Li J, Duncan SA. Generation of mice harbouring a conditional loss-of-function allele of Gata6. BMC developmental biology. 2006; 6:19. [PubMed: 16611361]

Song MR, Sun Y, Bryson A, Gill GN, Evans SM, Pfaff SL. Islet-to-LMO stoichiometries control the function of transcription complexes that specify motor neuron and V2a interneuron identity. Development (Cambridge, England). 2009; 136:2923–2932.

Tao H, Kawakami Y, Hui CC, Hopyan S. The two domain hypothesis of limb prepattern and its relevance to congenital limb anomalies. Wiley Interdiscip Rev Dev Biol. 2017

Yang L, Cai CL, Lin L, Qyang Y, Chung C, Monteiro RM, Mummery CL, Fishman GI, Cogen A, Evans S. Isl1Cre reveals a common Bmp pathway in heart and limb development. Development (Cambridge, England). 2006; 133:1575–1585.

Zhong Y, Wang Z, Fu B, Pan F, Yachida S, Dhara M, Albesiano E, Li L, Naito Y, Vilardell F, Cummings C, Martinelli P, Li A, Yonescu R, Ma Q, Griffin CA, Real FX, Iacobuzio-Donahue CA. GATA6 activates Wnt signaling in pancreatic cancer by negatively regulating the Wnt antagonist Dickkopf-1. PloS one. 2011; 6:e22129. [PubMed: 21811562]

Zhuang S, Zhang Q, Zhuang T, Evans SM, Liang X, Sun Y. Expression of Isl1 during mouse development. Gene Expr Patterns. 2013; 13:407–412. [PubMed: 23906961]

HIGHLIGHTS

- *Gata6* is transiently expressed in the anterior of nascent hindlimb buds.
- GATA6 binds to *Isl1* enhancer sequences located 3′ to the *Isl1* gene *in vitro*.
- *Gata6* and *Zfpn2* cooperate to repress transcription through the *Isl1* enhancer *in vitro*.
- Conditional knockout of *Gata6* results in upregulation of *Isl1* expression in the anterior of nascent hindlimb buds.

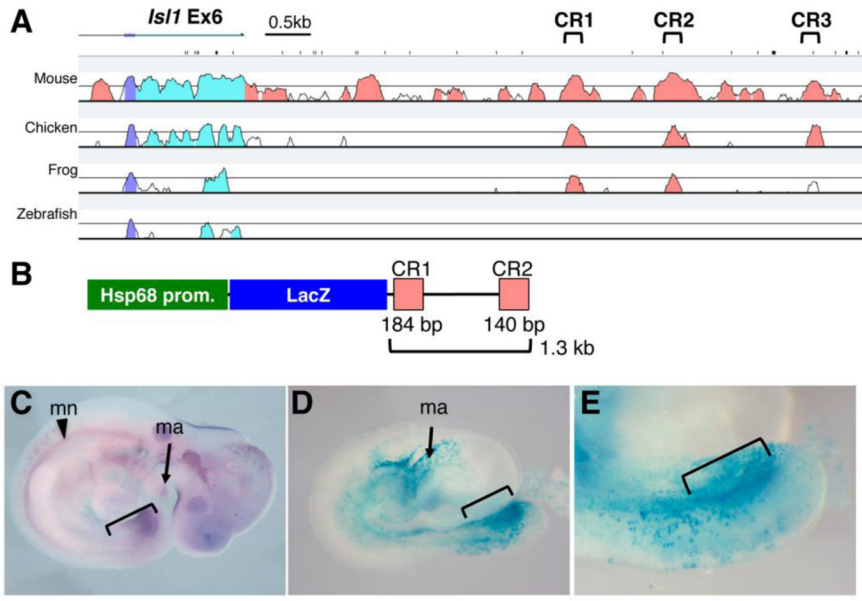

Figure 1. *Isl1* enhancer drives reporter expression in the hindlimb progenitors

(A) VISTA (http://pipeline.lbl.gov/) analysis shows conservation of human sequence (hg19) in mouse (mm10), chicken (galGal3) and frog (xenTro2), but not zebrafish (Zv9) in the 3′ region from the ISL1 gene. The CR1, CR2 and CR3 sequences are indicated. Purple and light blue peaks denote coding and 3′ UTR sequences, respectively, in the *Isl1* exon 6.

(B) Schematic presentation of the transgenic construct with the 1.3 kb region containing the CR1 and CR2 sequences. The 1.3 kb sequence contains the sequence between CR1 and CR2.

(C) *Isl1* expression pattern in a wild type embryo at E9.5.

(D, E) LacZ-stained embryo after injection of the transgenic construct. E shows close up of the hindlimb-forming region in D.

The bracket shows the hindlimb-forming region. ma: mandibular arch, mn: motor neuron.

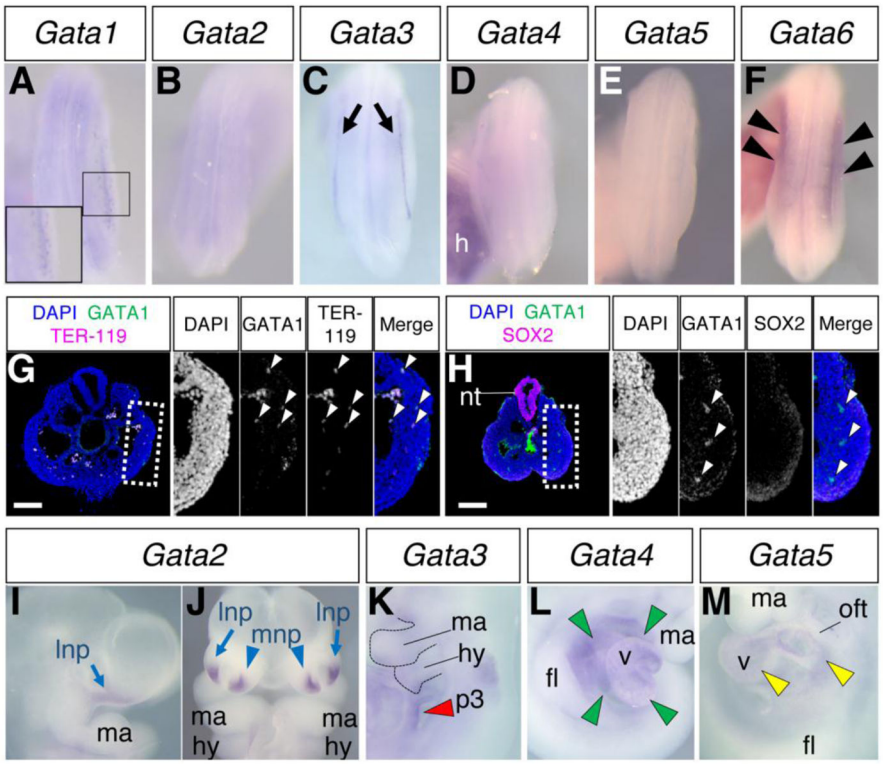

Figure 2. Expression patterns of *Isl1* and *Gata* genes

(A–F) Expression pattern of *Gata1* – *Gata6* at the 25/26 somite stage. The inset in A shows *Gata1* signals in putative hematopoietic cells. Shown are dorsal views of posterior part of the body. Arrows in C point to *Gata3* expression in the intermediate mesoderm. Arrowheads in F point to *Gata6* signals in the flank and the anterior hindlimb forming region.

(G, H) Immunofluorescence of GATA1 and TER-119 (G) and GATA1 and SOX2 (H). Dotted rectangles are shown as close-up of the lateral plate mesoderm. Single channel images are shown in black/white for better contrast. GATA1 positive signals and TER-119 positive signals overlap (arrowheads in G). GATA1 positive signals do not overlap with SOX2 signals (arrowheads in H). scale bar = 100 μm.

(I–M) Expression pattern of *Gata2* (I, J), *Gata3* (K), *Gata4* (L) and *Gata5* (M) at E9.5 (I, K–M) and E10.5 (J).

(I, J) Blue arrows and blue arrowheads point to *Gata2* signals in the lateral nasal prominence and medial nasal prominence, respectively.

(K) Red arrowheads point to *Gata3* signals in the 3rd pharyngeal pouch.

(L) Green arrowheads point to *Gata4* signals in the heart.

(M) Yellow arrowheads point to *Gata5* signals in the heart.

Abbreviations: fl: forelimb bud, h: heart, hy: hyoid arch, lnp: lateral nasal prominence, ma: mandibular arch, mnp: medial nasal prominence, nt: neural tube, oft: outflow tract, p3: 3rd pharyngeal pouch, v: ventricle,

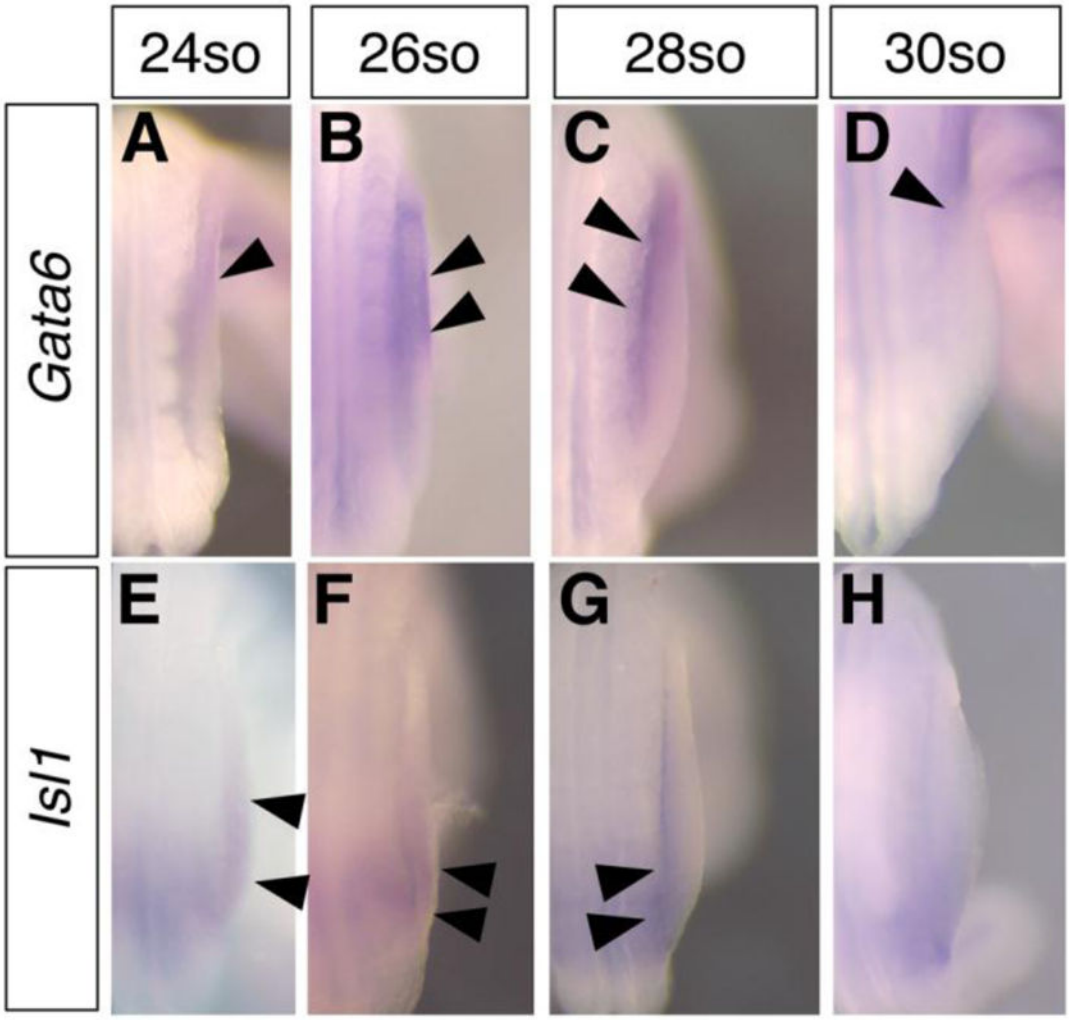

Figure 3. Comparison of expression patterns of *Gata6* and *Isl1*

(A–D) Dorsal views *Gata6* expression pattern in the hindlimb-forming region or the hindlimb bud at indicated stages. Arrowheads point to *Gata6* signals.

(E–H) Dorsal views *Isl1* expression pattern in the hindlimb-forming region or the hindlimb bud at indicated stages. Arrowheads point to *Isl1* signals.

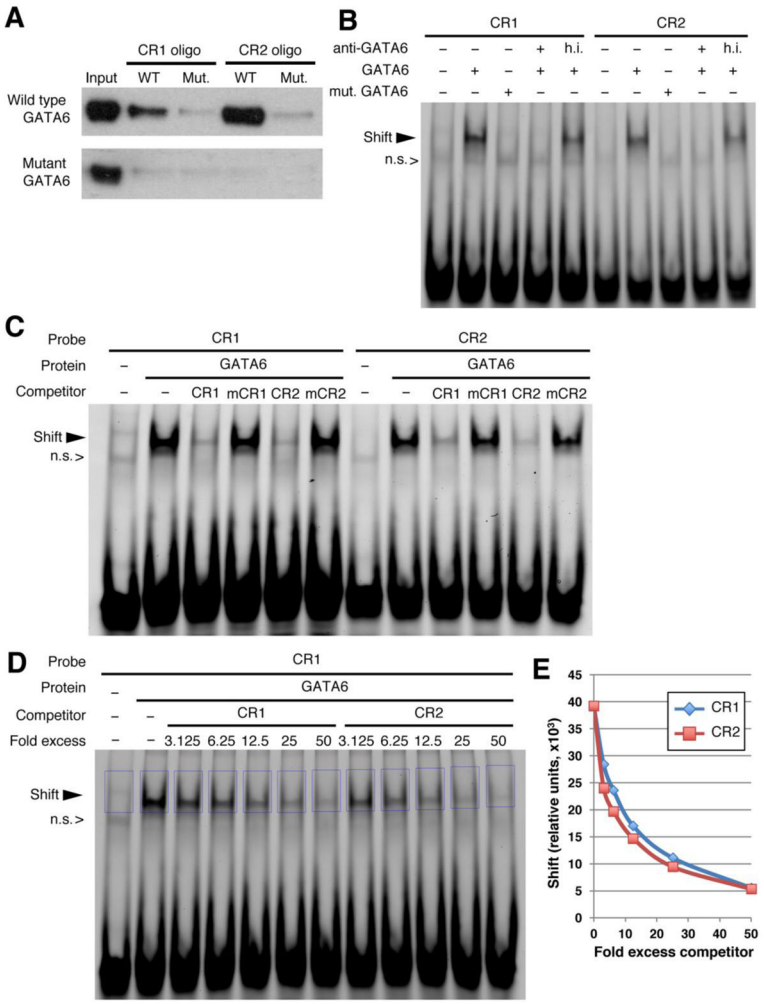

Figure 4. GATA6 binds to the GATA motif in the CR1 and CR2 sequences

(A) Double strand oligo DNA binding assay. GATA6 binds to both wild type CR1 and CR2 oligos, but not to oligos with mutations in GATA motifs (Mut.). Mutant GATA6 does not exhibit specific binding.

(B) EMSA assay showing a shift of CR1 oligos and CR2 oligos by GATA6. In vitro synthesized GATA6 protein shifts both CR1 and CR2 probes in the EMSA (indicated by an arrowhead), while mutant GATA6 does not produce a shift of either probe. The mobility shift produced by GATA6 was blocked by pre-incubation of GATA6 with anti-GATA6 antibody, but not by pre-incubation with heat-inactivated (h.i.) anti-GATA6 antibody. n.s.: non-specific.

(C) GATA6 binding to CR1 or CR2 probes can be blocked with cold competitor DNA containing wild-type CR1 or CR2 sequences, but not by competitors in which the GATA motif has been mutated. n.s.: non-specific.

(D) Relative affinities between CR1 and CR2. GATA6 and CR1 probe DNA are co-incubated with cold competitors at indicated fold excess amount. After resolving GATA6-CR1 probe complex, the intensity of the area indicated by blue boxes are measured.

(E) A graph representing quantification of GATA6-probe band signal intensity. The X axis represents fold excess competitors. Blue line and red line show signals by cold CR1 and cold CR2 competitors, respectively. The y-axis represents relative intensities of the band, depicted as red boxes in (D), compared to the box in the left-most lane where no GATA6 was added in the binding reaction. Signal intensities were slightly lower when CR2 was used as competitor than CR1.

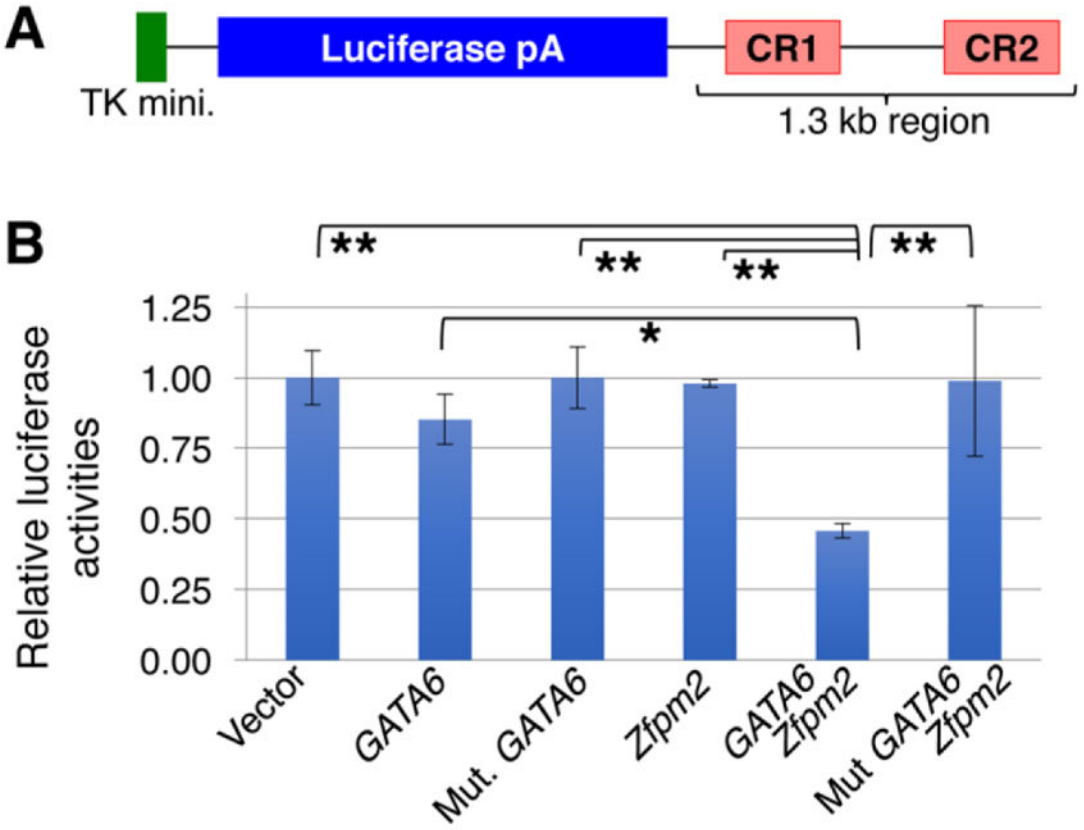

Figure 5. GATA6 synergizes with Zfpm2 to repress transcription in vitro

(A) Schematic presentation of the luciferase reporter construct with thymidine kinase minimum promoter (TK mini.) and the CR1-CR2 sequence. The 1.3 kb sequence contains both CR1, CR2 and the sequence between them.

(B) Luciferase reporter assay with indicated factors. *GATA6+Zfpn2* repressed the *Isl1*-luciferase. * $p<0.05$, ** $p<0.01$. Shown is a representative data from three independent experiments.

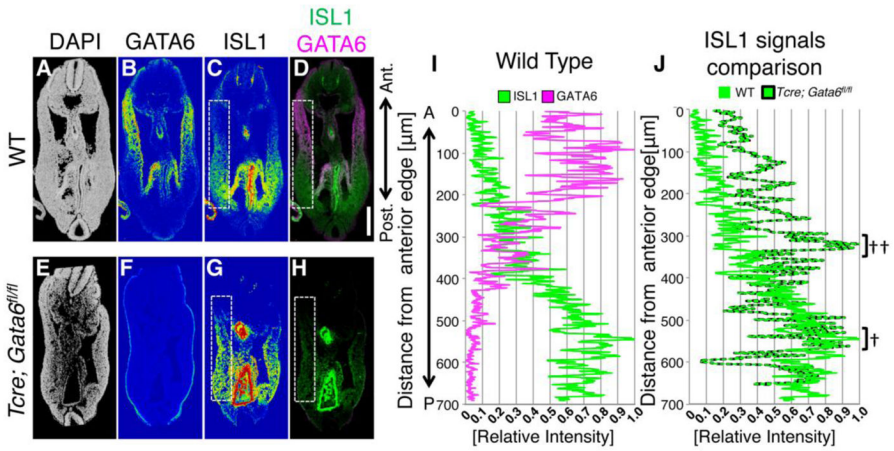

Figure 6. Immunofluorescence analysis of ISL1 signals in the nascent hindlimb bud

(A–H) Confocal images of the nascent hindlimb bud of the coronal section at the 28 somite stage. B, C, F and G are shown in rainbow color. Dotted areas in C, D, G and H show nascent hindlimb buds, where line scanning for ISL1 and GATA6 were performed. Scale bar: 200 μm.

(I) Relative fluorescent intensity of GATA6 (magenta) and ISL1 (green) along the anterior-posterior axis of the nascent hindlimb bud in wild type embryos. The highest signal intensity of ISL1 and GATA6 in the section is set as 1.0 intensity, and other signal intensities are relative to the highest signal intensity.

(J) Overlay of ISL1 signal intensity analysis along the anterior-posterior axis of the nascent hindlimb bud of wild type (green) and *Tcre; Gata6*$^{fl/fl}$ (green with black dotted line) embryos at 28 somite stage. The highest ISL1 signals in wild type or *Tcre; Gata6*$^{fl/fl}$ hindlimb are set at 1.0 intensity. Highest ISL1 signals are detected in more anterior regions in of *Tcre; Gata6*$^{fl/fl}$ hindlimb buds, compared to wild type. Note that this panel does not compare the *ISL1* signal intensity between wild type sections and *Tcre; Gata6*$^{fl/fl}$ sections. Brackets denote highest levels of ISL1 signals in wild type (†) and *Tcre; Gata6*$^{fl/fl}$ (††) embryos.

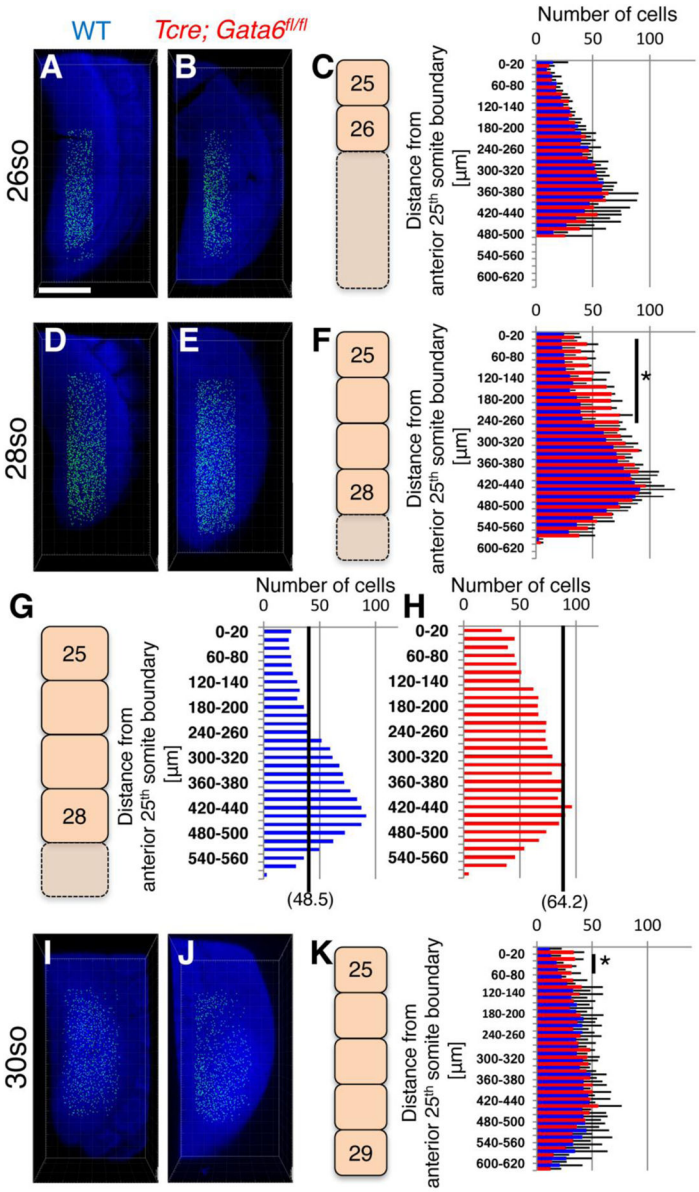

Figure 7. Greater number of cells express *Isl1* in *Tcre; Gata6$^{fl/fl}$*

(A, B, D, E, I, J) Confocal images of fluorescent *in situ* hybridization for *Isl1* intron probe. Lateral views with the dorsal side to the right are shown. Image stacks are analyzed as 3D image by Imaris software. Scale bar: 200 μm.

(C, F–H, K) Histogram for the number of *Isl1*-transcribing cells. The position and number of signals are defined by the spot function in Imaris. Solid lines in G and H show the average of frequencies (cell numbers). Left side of panels shows positions of somites, relative to the histogram. Solid bars with asterisk in F and K indicate that each of 20 μm domains in *Tcre; Gata6$^{fl/fl}$* section has greater number of *Isl1*-transcribing cells than wild type section by t-test ($p<0.05$). To decrease complexity of presentation, the pairs of wild type and *Tcre; Gata6$^{fl/fl}$*

with statistical differences are shown as a domain. The number in each column of histograms in C, F, G, H and K is the average of numbers from three embryos.